Petroleum Science 19 (2022) 663–677

Contents lists available at ScienceDirect

Petroleum Science

journal homepage: www.keaipublishing.com/en/journals/petroleum-science

Original Paper

Time-dependent borehole stability in hard-brittle shale

Chuan-Liang Yan [a, b], Lei-Feng Dong [b], Kai Zhao [c, *], Yuan-Fang Cheng [a, b], Xiao-Rong Li [d], Jin-Gen Deng [d], Zhen-Qi Li [b], Yong Chen [b]

[a] Key Laboratory of Unconventional Oil & Gas Development (China University of Petroleum (East China)), Ministry of Education, Qingdao, 266580, Shandong, China
[b] School of Petroleum Engineering, China University of Petroleum (East China), Qingdao, 266580, Shandong, China
[c] College of Petroleum Engineering, Xi'an Shiyou University, Xi'an, 710065, Shaanxi, China
[d] State Key Laboratory of Petroleum Resources and Prospecting, China University of Petroleum (Beijing), Beijing, 102249, China

ARTICLE INFO

Article history:
Received 19 November 2020
Accepted 25 November 2021
Available online 16 December 2021

Edited by Yan-Hua Sun

Keywords:
Shale
Rock damage
Drilling fluid density
Borehole stability

ABSTRACT

Rock damage appears in brittle shale even prior to peak stress (i.e., before failure) due to the occurrence of microcracks in these rocks. In this work, a coupled hydromechanical model was built by incorporating the mechanical and fluid seepage induced stresses around a wellbore during drilling. The borehole instability mechanism of hard-brittle shale was studied. The results show that even if a well is simply drilled into a hard-brittle shale formation, the formation around the borehole can be subjected to rock damage. The maximum failure ratio of the formation around the borehole increases with drilling time. A lower drilling fluid density corresponds to a faster increase in the failure ratio of the borehole with time and a shorter period of borehole collapse. When the initial drilling fluid density is too low, serious rock damage occurs in the formation around the borehole. Even though a high-density drilling fluid is used after drilling, long-term borehole stability is difficult to maintain. While drilling in hard-brittle shale, drilling fluid with a proper density should be used rather than increasing the density of the drilling fluid only after borehole collapse occurs, which is more favorable for maintaining long-term borehole stability.

1. Introduction

Borehole instability is a major problem that generally exists in oil and gas drilling and causes losses of more than 1×10^{10} dollars every year worldwide (Zeynali, 2012), and wasted time accounts for more than 40% of all non-drilling time (Dodson et al., 2004; Zhang et al., 2009; Yan et al., 2014). Severe borehole instability may even cause environmental disasters.

Borehole instability is mainly affected by the interaction of the mechanical properties of rocks and the chemical properties of the drilling fluid (Hale et al., 1993; Kanfar et al., 2015; Zhang et al., 2018). Previously, mechanical factors were mostly analyzed by focusing on the coupled effects of rock mechanics and porous fluid flow, while chemical factors were examined based on the hydration of shale. Before the 1970s, studies of these two aspects were carried out independently (Browning and Perricone, 1963; Fairhurst and Cook, 1966). From the 1970s to 1990s, these two aspects were gradually combined, but only in the experimental research area (Chenevert, 1970). Mechanical and chemical factors were not coupled in quantitative borehole stability analyses until the late 1990s (Yew et al., 1990; Mody and Hale, 1993). However, such studies were still limited to analyzing the influences of water contents on the mechanical parameters while considering chemical effects. Yu et al. (2001) and Chen et al. (2003) proposed a borehole stability model considering the coupled effect of fluid flow and chemical properties in an irreversible transfer process. Subsequently, studies of borehole stability with multifield coupling were expanded horizontally based on this method. A fully coupled mechanical-chemical model was developed to include multiple field factors: mechanics, chemistry, electric potential, and thermodynamics. For example, the coupled chemo-poro-thermoelastic model has been proposed to consider the effects of temperature, seepage, and hydration on the borehole stability of shale (Wang et al., 2006; Ghassemi et al., 2009). The coupled fluid-solid-chemistry model of borehole instability incorporates the fluid flow induced by electrochemical potential and ion diffusion as well as its effect on rock deformation (Wang et al., 2012). Recently,

* Corresponding author.
E-mail address: zkaiup@126.com (K. Zhao).

https://doi.org/10.1016/j.petsci.2021.12.019

borehole stability analysis has been expanded to bedding formations and comprehensively considers the combined effect of bedding planes and drilling fluid on borehole instability (Ma and Chen, 2015; Gao et al., 2017a; Yan et al., 2017b; Zhou et al., 2018).

Coupled multi-field studies have been maturely applied in the analysis of borehole stability in water-sensitive shale. However, the mechanism of borehole instability in hard-shale formations without obvious bedding planes is still not clearly understood.

Islam et al. (2009) established a wellbore stability model based on poroelastic constitutive model, coupled with pressure diffusivity formulation, to discuss a sensitivity analysis of the impact of shale intrinsic properties on transient pore pressure and its impact on time delayed borehole instability. Gao et al. (2017b) proposed an equivalent isotropic material model to solve the borehole stability in transversely isotropic formations. Through skillfully chosen material constants in the model, created a rule to correlate the behavior of transversely isotropic poroelastic model of borehole with the behavior of isotropic poroelastic model. Gao et al. (2020) proposed a semianalytical unsaturated poroelastic solution for an inclined borehole drilled through a formation saturated with two immiscible fluids.

Some hard-brittle shale has high strength and brittle behavior. During drilling, the borehole may collapse even if the drilling fluid pressure is higher than the collapse pressure and the concentrated stress does not reach the peak strength. In particular, the water sensitivity of such formations is weak. Borehole instability still shows strong time-dependent features.

In the loading and unloading process, the failure of brittle rocks is mainly caused by crack initiation, propagation, interaction and connection, representing a main failure mode of hard-brittle rocks (Yan et al., 2015; Eberhardt et al., 1999). In other words, brittle rocks are subjected to rock damage even prior to peak stress, and the failure is mainly caused by constant accumulation of rock damage. Therefore, to study the borehole instability of hard-brittle shale, the prepeak damage characteristics of formations must be studied.

Because the presence of damage-induced fractures reduces the effective bearing area for the loading of formation, the circumferential stress in rocks around the borehole increases such that the density of the drilling fluid required to maintain borehole stability is higher (Liu et al., 1998). Shao and Khazraei (1994) studied borehole stability under uniform and nonuniform *in situ* stresses with several material models, such as the Laderock elastic-plastic model, Lemaitre isotropic damage model, Costin anisotropic damage model and linear elastic model. The results demonstrate that the borehole wall analyzed from the Costin model is most likely to be unstable, followed by the Laderock model, while that from the Lamaitre model is the most difficult to damage.

By combining the microscopic damage and fracture mechanism, Zheng (2005) and Tang et al. (2007) established a model for calculating collapse and fracture pressures during drilling. They examined the initiation-condition and expansion-direction of microcracks around the borehole based on the damage mechanism of brittle formation. They predicted the pressure at the initial damage condition and analyzed the damage field of the formation around the borehole. Furthermore, they obtained the range of the damaged zone and the relationship between the stress distribution and the geomechanical characteristics of the formation in the damaged zone. However, their research does not consider the effect of rock damage (prior to peak strength) on the permeability evolution and the interaction between damaged shale and drilling fluid, which shows large deviations within drilling practice.

The failure process of brittle rocks includes the generation, propagation and accumulation of internal cracks. Microcracks caused by these stress disturbances can change the permeability characteristics of rocks and increase the seepage of drilling fluid into formations. On the one hand, microcracks change the physical and mechanical properties of hard-brittle shale, resulting in a gradual decrease in the strength of the formation. On the other hand, microcracks change the pore pressure in the formation, which changes the stress field around the borehole. Both a decrease in rock strength and an increase in the stress field can increase rock damage and result in an increased permeability and pore pressure distribution, thus leading to a higher risk of borehole collapse. Such interaction induced borehole collapse is a very common accident during drilling in hard-brittle shale. Therefore, the coupled hydromechanical model must be used to analyze the borehole instability of hard-brittle shale. In the previous borehole stability models that considered stress damage, the impact of the chemical effect on the strength of damaged shale was not considered. The coupling effect of stress-damage-seepage and drilling fluid chemical effect on shale strength is comprehensively considered in the borehole stability model in this paper to clarify the borehole instability mechanism of hard-brittle shale.

2. Borehole stability model of hard-brittle shale

Brittle shale mainly undergoes elastic deformation and brittle failure during the loading process, and plastic deformation and damage before peak failure are small. However, the clay content of brittle shale is relatively high, and the borehole wall is in the high-pressure drilling fluid environment during drilling. Even there is a small damage in shale, damage cracks will be expanded under the effect of high pressure of drilling fluids, and the damage continues to accumulate. Eventually, it is easy to cause the failure of the borehole wall rock.

2.1. CWFS model

From the perspective of mechanics, brittle rock failure is a process in which rock strength gradually decreases (Walton, 2019). The number of microcracks in a rock increases from the initial stage of failure, such that the cohesive force between the particles of the rock gradually decreases or disappears, resulting in a decline in the cohesive strength of the rock. With the continuous expansion and connection of microcracks, and ultimately the appearance of macrocracks, a friction force between microcrack surfaces gradually emerges under the combined action of normal stress and shear stress, resulting in a gradual increase in the overall friction strength of the rock. Finally, the cohesion and friction strength of hard-brittle rock will each tend toward a fixed value, at this time the rock is stable at the residual strength (Hajiabdolmajid et al., 2002; Hajiabdolmajid and Kaiser, 2003; Walton, 2019).

Based on the characteristics of brittle rock where the cohesive strength continuously weakens and the friction strength gradually increases during the failure process, Hajiabdolmajid and his coworkers (Hajiabdolmajid et al., 2002; Hajiabdolmajid and Kaiser, 2003) proposed a constitutive model of cohesion weakening and frictional strengthening (CWFS) based on the Mohr-Coulomb strength criterion to describe the failure of hard-brittle rocks (Fig. 1). The model assumes that the cohesion and friction strength of brittle rocks are functions of plastic strain. The cohesion of the rock controls the bond strength between its particles at the beginning of loading. At this time, the initial cohesion strength of the rock reaches the maximum value and the friction strength of the rock is 0. As the stress increases, cracks begin to occur in the rock, the cohesive strength gradually decreases, and the friction strength gradually increases and is ultimately controlled. Finally, the friction strength and residual cohesion of the rock tend toward a fixed value, that is, the residual strength after the rock reaches peak failure. The research results show that the CWFS model has a

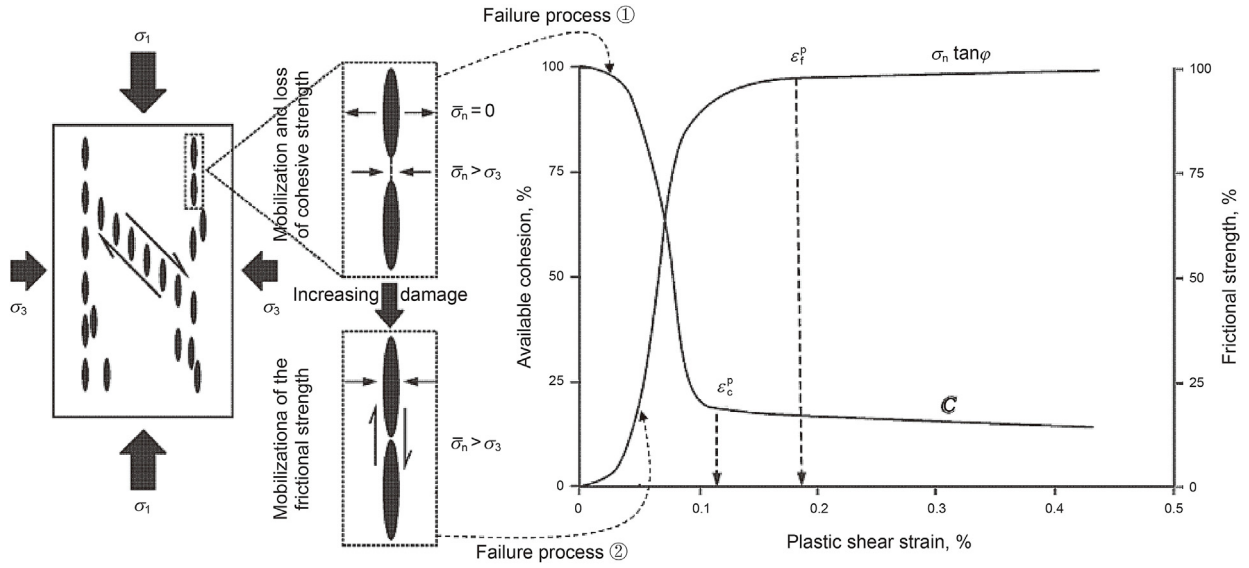

Fig. 1. Schematic diagram of the relationship between cohesion, friction strength and plastic strain (ε_f^p and ε_c^p are the plastic strains when cohesion and friction strength reach the final fixed values, respectively) (Hajiabdolmajid et al., 2002).

good effect on the simulation of the brittle failure range and depth of hard rock under high ground stress (Hajiabdolmajid et al., 2002; Hajiabdolmajid and Kaiser, 2003; Su, 2006; Qiao et al., 2012; Renani and Martin, 2018).

The CWFS model is expressed as follows:

$$f(\sigma) = \tau_0 = C(\varepsilon^p) + \sigma_n \tan\varphi(\varepsilon^p) \tag{1}$$

where τ_0 is the shear strength of the formation; C and φ are the cohesion strength and the angle of internal friction of the formation, respectively; ε^p is the equivalent plastic strain; and σ_n is the effective normal stress on the failure surface of the formation.

When the effective stress exceeds the yield stress of the formation, the rock around the well will undergo plastic deformation. The equivalent plastic strain calculation formula is:

$$\varepsilon^p = \frac{\sqrt{2}}{3}\sqrt{\left(\varepsilon^{p1} - \varepsilon^{p2}\right)^2 + \left(\varepsilon^{p2} - \varepsilon^{p3}\right)^2 + \left(\varepsilon^{p3} - \varepsilon^{p1}\right)^2} \tag{2}$$

where ε^{p1}, ε^{p2} and ε^{p3} are the principal plastic strains in three directions, respectively.

Hajiabdolmajid et al. (2002) proposed that the original intention of the CWFS model is to calculate the collapse range and size of brittle rock tunnels. Therefore, the proposed model focuses on the full stress-strain process of rock. For hard-brittle shale, the bearing capacity of the core decreases rapidly after reaching the peak strength during the loading process, and the residual strength is extremely low. During the drilling process, which is affected by high-speed circulation of the drilling fluid, the hard-brittle shale will quickly break and lose its bearing capacity after reaching the peak stress. The damaged rock will be quickly washed away by the high-speed flowing drilling fluid and peel off from the well wall. Since the formation is hard and brittle and the water sensitivity is weak, these collapsed blocks are difficult to destroy in the drilling fluid, and serious jamming accidents easily occur during the tripping process. Therefore, when drilling in hard-brittle shale formations, the stress on the borehole wall must always be maintained below the peak strength to ensure safe drilling. To better describe the constitutive characteristics of hard-brittle shale before the peak, and more easily select model parameters, the CWFS model is modified. The relationship between cohesion, internal friction angle and plastic strain is limited to the peak strength to better describe the prepeak constitutive characteristics of hard-brittle shale, and facilitate acquisition of the parameters (Yan et al., 2017a).

$$C(\varepsilon^p) = \begin{cases} C_i & \varepsilon^p = 0 \\ C_i - \left(\dfrac{\varepsilon^p}{\varepsilon^{pe}}\right)^m (C_i - C_e) & 0 \le \varepsilon^p \le \varepsilon^{pe} \\ 0 & \varepsilon^p > \varepsilon^{pe} \end{cases} \tag{3}$$

$$\varphi(\varepsilon^p) = \begin{cases} C_i & \varepsilon^p = 0 \\ \varphi_e \left(\dfrac{\varepsilon^p}{\varepsilon^{pe}}\right)^n & 0 \le \varepsilon^p \le \varepsilon^{pe} \\ 0 & \varepsilon^p > \varepsilon^{pe} \end{cases} \tag{4}$$

where C_i is the initial cohesive strength of hard-brittle shale; ε^{pe} is the equivalent plastic strain when the formation reaches peak failure; C_e is the cohesion strength when the formation reaches peak failure; φ_e is the internal friction angle when the formation reaches peak failure; and m and n are constants related to the mechanical properties of the materials, $m = 2$ and $n = 0.6$ are used in this paper.

Assuming that the brittle rock satisfies equation $\varphi = 0$ at the initial stage of loading, the initial cohesive strength C_i is 1/2 of the rock cracking strength. Since damage to the hard-brittle shale is not obvious before the linear elastic stage, for facilitating calculation, we believe that cracks in the hard-brittle shale start to develop from the linear elastic stage, that is, C_i is 1/2 of the ultimate elastic strength. The cohesive force C_e and the internal friction angle φ_e during rock failure can be obtained through the results of conventional uniaxial and triaxial strength experiments.

2.2. Elastic-plastic damage model

The plasticity of rock materials refers to frictional sliding between fracture surfaces in rocks, while rock damage indicates the

initiation and propagation process of internal cracks (Jia et al., 2009). In the stress loading process, damage indicates that the effective bearing area of rocks is reduced. According to the plasticity-damage coupling theory, 1) plasticity and damage affect each other through their potential functions, and 2) the coupled effect of plasticity and damage is generated through the evolution of their internal variables (Shen et al., 2001). To study the degree and range of hard-brittle shale formation damage under different drilling mud densities, a damage evolution model of hard-brittle shale formations based on plastic strain was built.

For formations with rock damage, the microstructure of the formation can change, which changes the material state and macroscopic mechanical properties of the formation, thus causing the mechanical characteristics of the formation to vary accordingly with damage (Jia et al., 2009). To apply the plastic damage model of hard-brittle shale formations to the analysis of borehole stability, the damage variable and its evolution law should be defined. In this work, the assumptions of damage variables are simplified as follows (Yang et al., 2000): hard-brittle shale formations are intact before drilling, and the proportion of damaged materials in formation gradually increases with the development of plastic deformation; the damage variable of formation is related only to the history of plastic deformation.

The total deformation of hard-brittle shale formations consists of elastic deformation, plastic deformation and damage deformation. The elastic-plastic damage model can be expressed as:

$$\{\mathrm{d}\varepsilon\} = \{\mathrm{d}\varepsilon^{\mathrm{p}}\} + \left\{\mathrm{d}\varepsilon^{\mathrm{d}}\right\} + \{\mathrm{d}\varepsilon^{\mathrm{e}}\} \tag{5}$$

where $\{\mathrm{d}\varepsilon\}$, $\{\mathrm{d}\varepsilon^{\mathrm{p}}\}$, $\{\mathrm{d}\varepsilon^{\mathrm{d}}\}$, and $\{\mathrm{d}\varepsilon^{\mathrm{e}}\}$ represent the total strain, plastic strain, damage strain, and elastic strain of the formation rock during drilling, respectively.

The relationship between the increment of elastic stress and elastic strain is determined by the elastic stiffness matrix, and the increment of elastic strain can be expressed as:

$$\{\mathrm{d}\varepsilon^{\mathrm{e}}\} = [E^*]^{-1}\{\mathrm{d}\sigma\} \tag{6}$$

with

$$[E^*] = [E^*]^{-1}\{\mathrm{d}\sigma\} \tag{7}$$

where $[E^*]$ is the elastic stiffness matrix; $[E]$ is the elastic constitutive matrix under an undamaged state. Under three-dimensional (3D) coordinates, the elastic matrix is a symmetrical 6×6 matrix containing 36 components. Moreover, $\{\mathrm{d}\sigma\}$ and D_{d} represent the stress increment matrix and the stress damage factor during loading on the formation, respectively.

The increment of the plastic strain of the formation is determined according to plastic potential theory. From the perspective of damage mechanics, the yield function and potential function of a damaged formation can be separately defined as follows:

$$F(\sigma, H(\chi), D_{\mathrm{d}}) = 0 \tag{8}$$

$$G(\sigma, H(\chi), D_{\mathrm{d}}) = 0 \tag{9}$$

where $F()$, $G()$ and σ indicate the yield function, plastic potential function and stress of a formation, respectively; χ is the scalar of the internal variable for describing the equivalent plastic strain of the formation; $H()$ refers to the function of the internal variable χ and is used to characterize the hardening or softening characteristics of the formation when plastic deformation develops in the formation.

In hard-brittle shale formations, plastic deformation and formation damage are assumed to appear simultaneously; then, the expressions of plastic strain and damage strain are shown as follows:

$$\{\mathrm{d}\varepsilon^{\mathrm{p}}\} + \left\{\mathrm{d}\varepsilon^{\mathrm{d}}\right\} = \lambda\left\{\frac{\partial G(\sigma, H(\chi), D_{\mathrm{d}})}{\partial\sigma}\right\} \tag{10}$$

where λ is related to the hardening laws of the formation, and the specific value can be determined according to the following equation.

$$\lambda = \frac{\left\{\frac{\partial F}{\partial\sigma}\right\}^{\mathrm{T}}[E^*]\{\mathrm{d}\varepsilon\}}{\left\{\frac{\partial F}{\partial\sigma}\right\}^{\mathrm{T}}[E^*]\left\{\frac{\partial G}{\partial\sigma}\right\} - A} \tag{11}$$

where A represents the hardening parameter of the formation.

When the effective stress in the formation is $\{\mathrm{d}\sigma\}$, the loading condition under the plastic state is

$$F(\{\sigma\}, k) = 0 \tag{12}$$

where k is correlated with the plastic strain of the formation. In hardening materials, k equals the plastic work performed by the formation in the generation of plastic deformation.

$$\mathrm{d}k = \{\sigma\}^{\mathrm{T}}\{\mathrm{d}\varepsilon^{\mathrm{p}}\} = \lambda\{\sigma\}^{\mathrm{T}}\left\{\frac{\partial G}{\partial\sigma}\right\} \tag{13}$$

Based on classical elastic-plastic mechanics theory, the plastic constitutive matrix of damaged formations can be obtained as follows:

$$\left[E^{\mathrm{p}*}\right] = \frac{[E^*]\left\{\frac{\partial G}{\partial\sigma}\right\}\left\{\frac{\partial F}{\partial\sigma}\right\}^{\mathrm{T}}[E^*]}{\left\{\frac{\partial F}{\partial\sigma}\right\}^{\mathrm{T}}[E^*]\left\{\frac{\partial G}{\partial\sigma}\right\} - A} \tag{14}$$

2.3. Effective stress principle

Hard-brittle shale is a porous medium consisting of a solid matrix and fluids in pores. Deformation and failure of rocks are mainly influenced by effective stress. According to Biot's effective stress theory, Eq. (11) can be obtained.

$$\sigma_{\mathrm{ij}}{}' = \sigma_{\mathrm{ij}} - \alpha P_{\mathrm{p}}\delta_{\mathrm{ij}} \tag{15}$$

where σ_{ij} and $\sigma_{\mathrm{ij}}{}'$ refer to the components of total stress and effective stress on rocks around the borehole, respectively; and P_{p}, δ_{ij} and α denote the pore pressure, Kronecker symbol and coefficient of effective stress, respectively, α is defined as follows:

$$\alpha = 1 - \frac{K_{\mathrm{V}}}{K_{\mathrm{S}}} \tag{16}$$

where K_{V} represents the compressive modulus of the volume of rocks in the formation; K_{S} refers to the compressive modulus of solid matrix particles in rocks.

2.4. Equation for the damage evolution of hard-brittle shale

Hard-brittle shale is assumed to be subjected to rock damage only during plastic deformation rather than in the elastic state. Furthermore, damage to and plastic deformation of a formation appear simultaneously. The relationship between the damage

factor and equivalent plastic strain of hard-brittle shale formations is a first-order exponential attenuation function. Therefore, the relationship between the normalized damage factor and normalized equivalent plastic strain is shown as follows:

$$D = A_0 \exp\left(\frac{-\varepsilon^{pn}}{a}\right) + B_0 \tag{17}$$

$$A_0 = \frac{1}{\exp\left(-\frac{1}{a}\right) - 1} \tag{18}$$

$$B_0 = -\frac{1}{\exp\left(-\frac{1}{a}\right) - 1} \tag{19}$$

where D represents the normalized damage factor. When $D = 1$, the stress of rocks reaches the peak strength and failure occurs; when $D = 0$, no damage occurs in the formation. In addition, a indicates the material parameter of hard-brittle shale, which can be determined through experiments; ε^{pn} represents the normalized equivalent plastic strain and can be expressed as follows:

$$\varepsilon^{pn} = \frac{\varepsilon^{p}}{\varepsilon^{pe}} \tag{20}$$

2.5. Evolution equation for the permeability of hard-brittle shale

In the compressive test, the failure of brittle rocks results from the initiation, propagation and connection of microcracks in the loading process. After microcrack initiation, even if stress does not reach the peak strength, the permeability of rocks gradually increases (Fig. 2) (Souley et al., 2001). The permeability of intact hard-brittle shale formations is very low, and stress slightly affects seepage. However, for damaged formations, new damage appears in the formation due to the interaction of stress and pore pressure on microcracks. In addition, with the constant accumulation of formation damage, more microcracks are generated, and the interactions of seepage, stress and damage are magnified.

Shale typically has a high porosity and low permeability, and the porosity of some shales can reach approximately 40%, while the permeability is very low (Jia, 2009). In the petroleum industry, the porosity of connected pores is generally known as the effective porosity. Although the total porosity of shale formations is high, the connectivity between pores is poor. Therefore, the effective porosity and permeability are extremely low. When the stress state of the formation changes considerably, microcracks appear inside the rocks due to stress damage such that the closed pores become connected with each other. Although the volume of new cracks is not large, they all connect the pores and channels, which significantly increases the corresponding porosity of the connected pores and channels in shale.

The permeability of brittle granite (with low permeability) before peak failure can reach a value of more than a thousand times that before loading (Souley et al., 2001; Oda et al., 2002). By testing the permeability of shale in the loading process, Jiang et al. (Jiang et al., 2002) obtained a similar result in that the permeability of shale before peak failure substantially increased.

In previous studies of wellbore instability, permeability of a formation around a borehole was generally expected to remain unchanged, although it was practically changed when drilling a borehole. The permeability of damaged formations evolves in accordance with the cubic law of seepage (Jia, 2009).

$$k = k_0(1 - D) + k_D D\left(1 + \varepsilon_v^{PF}\right)^3 \tag{21}$$

where k_0 and k_D indicate the permeability of an intact formation and the damaged formation, respectively; ε_v^{PF} represents the volumetric strain of the damaged section, which can be calculated as

$$\varepsilon_v^{PF} = D\varepsilon_v^{P} \tag{22}$$

where ε_v^{P} denotes the plastic volumetric strain.

2.6. Borehole instability criterion of hard-brittle shale

Borehole collapse is generally considered to be the result of shear failure, which is caused by a large difference between the concentrated tangential and radial stresses around the wellbore

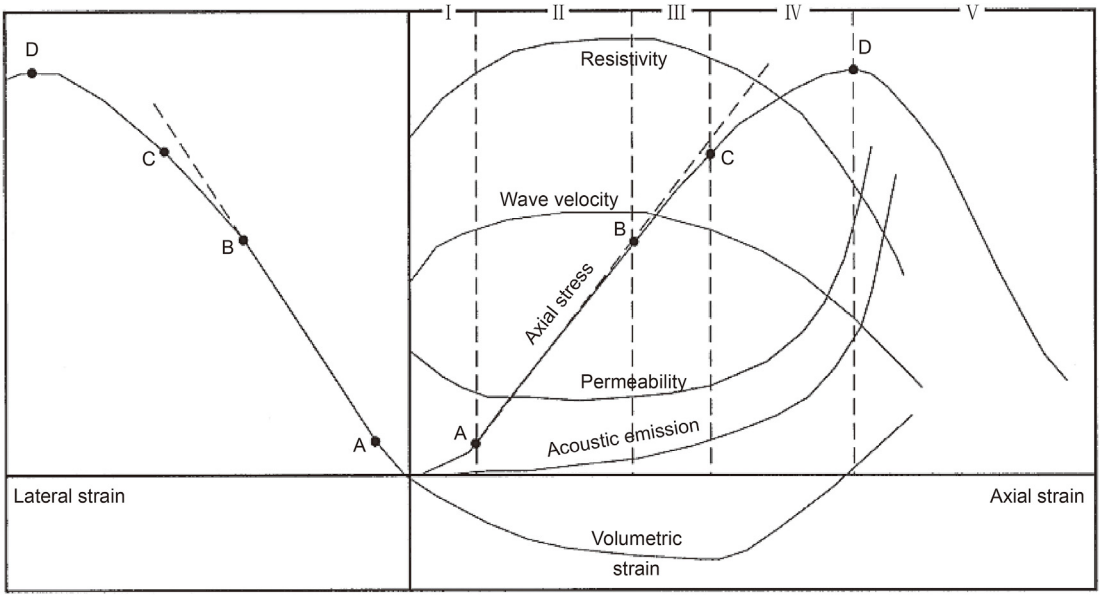

Fig. 2. Schematic of the physical property change in rock in the loading process (Souley et al., 2001).

due to low drilling fluid density. In general, in the cylindrical coordinate system of a borehole, three principal stresses around the borehole have the following laws when the borehole wall collapses (Chen et al., 2008).

(1) Vertical stress. With an increase in the distance from the wellbore wall to the far field formation, the vertical stress along the orientation of the maximum horizontal stress gradually increases, while that along the orientation of the minimum horizontal stress gradually decreases. In a formation far from a borehole, the vertical stress in each direction is eventually equal to the overburden pressure of the formation.
(2) Radial stress. Radial stress is generally the smallest principal stress on the borehole wall when borehole collapse occurs. With an increase in the distance from the wellbore wall to the formation, the radial stress in each direction gradually increases.
(3) Tangential stress. Tangential stress is generally the largest principal stress on the borehole wall when borehole collapse occurs. As the radial distance increases, the tangential stress in each orientation gradually decreases. Tangential stress has a maximum value on the wellbore wall along the orientation of the minimum horizontal stress and a minimum value at the orientation of the maximum horizontal stress. On the borehole wall at the orientation of the minimum horizontal *in situ* stress, the circumferential stress is maximal, and the difference between the circumferential stress and radial stress is the largest. Borehole instability generally appears at this position, and an ellipse-shaped borehole is finally formed (Zoback et al., 1985), as demonstrated in Fig. 3.

In this study, the Mohr-Coulomb criterion is applied to define the shear failure of rocks in the borehole wall. The criterion is represented by the principal stresses as shown in Eq. (20) (Chen et al., 2008). When the concentrated maximum and minimum principal stresses on the wellbore wall exceed the rock strength, shear failure occurs on the wellbore wall.

$$\sigma_1 = \sigma_3 \tan^2\left(\frac{\pi}{4}+\frac{\varphi}{2}\right) + 2C\tan\left(\frac{\pi}{4}+\frac{\varphi}{2}\right) \tag{23}$$

where σ_1 and σ_3 indicate the maximum and minimum effective principal stresses, respectively; φ and C represent the friction angle and cohesion of the rocks, respectively.

In hard-brittle shale, the damage states and changes in the permeability of the formation around the borehole vary under different drilling fluid densities, and the change laws of the pore pressure around the borehole and the strength of the formation relative to the soaking time in drilling fluid are closely related to the density of the drilling fluid. For these reasons, the variation laws of the collapse pressure with time are distinct when using different drilling fluids to drill a well. Therefore, obtaining time-dependent laws of explicit collapse pressure is difficult. To study the time effects of borehole stability in hard-brittle shale formations, according to the Mohr-Coulomb strength criterion, the concept of the failure ratio of rocks around a borehole wall is introduced to determine whether a borehole wall is stable. The failure ratio of the formation is defined as follows:

$$K = \frac{\sigma_1}{\sigma_3 \tan^2\left(\frac{\pi}{4}+\frac{\varphi}{2}\right) + 2C\tan\left(\frac{\pi}{4}+\frac{\varphi}{2}\right)} \tag{24}$$

where K represents the failure ratio of a formation.

By substituting the principal stresses of the formation around the borehole into the above equation, the failure ratio of the formation can be obtained. A failure ratio equal to 1 indicates that shear failure appears in the formation and that the borehole becomes unstable. When the failure ratio is smaller than 1, the borehole wall is still stable. A smaller failure ratio indicates better borehole stability. The failure ratio is used to characterize borehole stability in this study.

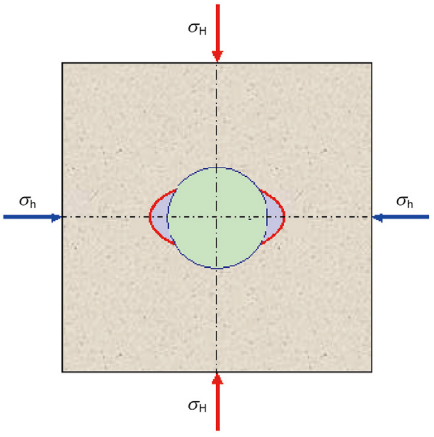

Fig. 3. Schematic diagram of borehole instability.

3. Time-dependent strength of hard-brittle shale

After drilling, the drilling fluid and filtrate invade the formation. Water-sensitive shale formations can become hydrated by the infiltrated drilling fluid, thus generating expansion stress. Moreover, the strength of a formation gradually decreases with increasing soaking time. In hard-brittle shale formations, the content of water-sensitive minerals is extremely low, and the presence of chemical inertness between the drilling fluid and rock substrates does not easily cause hydration of the formation. Therefore, the strength of the formation is only slightly affected by the drilling fluid. However, in the loading process of hard-brittle shale, microcracks constantly appear, leading to different stress states, numbers and volumes of microcracks. While drilling, the stresses around the borehole are redistributed, and stress concentration occurs. The stress state of hard-brittle shale deeply buried underground changes in this process, which easily causes stress damage. At this time, the drilling fluid infiltrates into the formation along the microcracks induced by stress damage, which influences the mechanical properties of hard-brittle shale. The influences of drilling fluid infiltration on damaged hard-brittle shale are mainly shown demonstrated as follows: first, drilling fluid infiltration increases the fluid pressure. Second, drilling fluid infiltration changes the properties of fracture planes in shale and lubricates the fracture planes. Moreover, such infiltration decreases the friction strength of the microcrack planes and the fracture toughness at the tips of the microcracks, which results in higher stress being transferred to the tips of the cracks and accelerates further propagation of microcracks. The interaction of these two aspects leads to the phenomenon that the strength of damaged shale weakens with time, and the decrease in the amplitude of strength after hard-brittle shale comes in contact with drilling fluid is closely correlated with the damage degree of rocks.

To study the influence laws of drilling fluid on the strength of hard-brittle shale under different stress states, rock cores were divided into five groups. Among them, one group of rock cores was directly soaked in the drilling fluid, while the other four groups

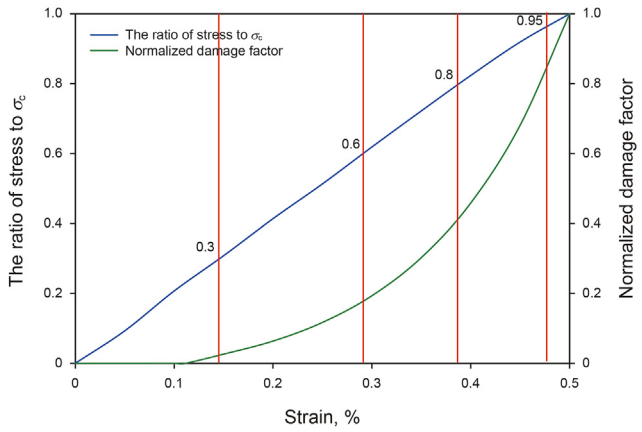

Fig. 4. Schematic diagram of load stress and normalized damage factors (Yan, 2014; Wang et al., 2016a).

were first compressed under loads equivalent to 30%, 60%, 80% and 95% of the uniaxial compressive strength (σ_c) under uniaxial conditions and then soaked in drilling fluid (Wang et al., 2016a). The aim is to test the σ_c of each group of rock cores after soaking for a certain time. Different loading stresses can induce distinct degrees of stress damage (as displayed in Fig. 4). On this basis, the influence laws of the interaction of the stress damage and drilling fluid on the strength of hard-brittle shale were studied.

Based on the above experimental method, the σ_c of each group of hard-brittle shale cores after soaking in drilling fluid for 48, 96 and 168 h were obtained. The average σ_c of the samples without soaking in drilling fluid was 83.1 MPa.

Fig. 5 presents a comparison of the σ_c of the shale cores as a function of the soaking time in drilling fluid after loading under different stresses. As shown by the experimental results, as the soaking time in the drilling fluid increased, the σ_c of hard-brittle shale gradually decreased. The decrease rate is the maximum at the beginning and then gradually reduces and finally tends to be gradual. After hard-brittle shale has been in contact with the drilling fluid for one week, the σ_c is basically no longer affected by the soaking time. Before soaking, the cores with different stress damages are affected differently by soaking in the drilling fluid, and greater stress damage corresponds to a larger decrease in the amplitude of the σ_c after soaking. For the cores that were not subjected to stress loading before soaking, the σ_c is reduced by approximately 12% after soaking for seven days, indicating that hard-brittle shale has weak water sensitivity and is slightly affected

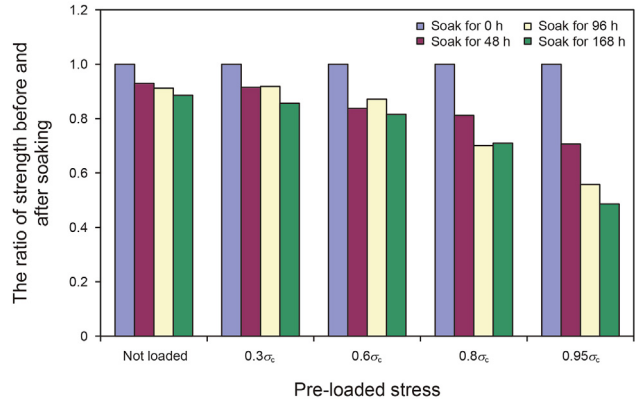

Fig. 5. Comparison of the strength of hard-brittle shale after soaking in the drilling fluid (Yan, 2014).

by the drilling fluid in the intact state. The uniaxial strengths of the cores compressed by a stress equivalent to 30%, 60%, 80% and 95% of the σ_c before soaking decreased by 14%, 18%, 29% and 52% after soaking for seven days, respectively. Obviously, when the stress applied before soaking is low, the stress damage exerts a small influence on the decrease in the amplitude of the σ_c of hard-brittle shale. However, once the loading stress exceeds a certain limit, the decrease in the amplitude of the σ_c grows rapidly.

When hard-brittle shale is contacted by drilling fluid, driven by physical and chemical reactions, such as the chemical potential and capillary force, the drilling fluid infiltrates into the interior of the rocks along microcracks, thereby changing the properties of the microcracks such that the σ_c of rocks gradually decreases with increasing soaking time. After saturation with the filtrate of the drilling fluid, the shale stops absorbing water, and the σ_c of the formation decreases slowly under these conditions. The decrease in the amplitude of the σ_c of shale is not only affected by the soaking time in the drilling fluid but is also correlated with the stress state of the cores before soaking. Moreover, this decrease is related to the stress damage degree in the cores. Therefore, the effect of the damage factor must be introduced in the influence laws of the drilling fluid on the σ_c of hard-brittle shale.

$$\sigma_c(t,D) = \sigma_{cl} - A \cdot f(D) \exp\left(-\frac{B}{t}\right) \tag{25}$$

$$f(D) = C \cdot \exp(E \cdot D) \tag{26}$$

$$D = \frac{D_d}{D_f} \tag{27}$$

According to the experimental results, the change law of the σ_c of hard-brittle shale with soaking time in drilling fluid is shown as follows.

$$\sigma_c(t,D) = \sigma_{cl} - 10.3\exp(1.52 \cdot D)\exp\left(-\frac{15.7}{t}\right) \tag{28}$$

where $\sigma_c(t,D)$ and σ_{cl} represent the strength of the formation at moment t after drilling and the original strength of the formation before drilling, respectively; A, B, C and E are constants related to the formation properties and physical and chemical properties of the drilling fluid; D_d, D_f and D indicate the stress damage factor when the formation comes into contact with the drilling fluid, the damage factor when the load reaches the peak stress of the formation and the normalized stress damage factor, respectively; t refers to the contact time of the drilling fluid with the formation around the borehole.

4. Damage of hard-brittle shale after drilling

Finite element models had been used to study the formation damage and multi-physical field coupling around the wellbore by some researchers, and achieved good results. Gaede et al. (2013) proposed a constitutive model, based on non-equilibrium thermodynamics, that accounts for anisotropic damage distribution, anisotropic damage threshold and anisotropic damage evolution, and implemented this constitutive model using the finite element method, to calculate stress–strain curves and borehole stresses. Wang et al. (2016b, 2017a, 2017b) obtained the wellbore failure characteristics by proposing a finite element analysis technology by hydraulic-mechanical-chemical-damage coupling for wellbore stability analysis of transversely isotropic rock, and calculated the time-dependent collapse and fracture pressure of laminated rock. Ma and Zhao (2018) proposed a dual-porosity finite-element model

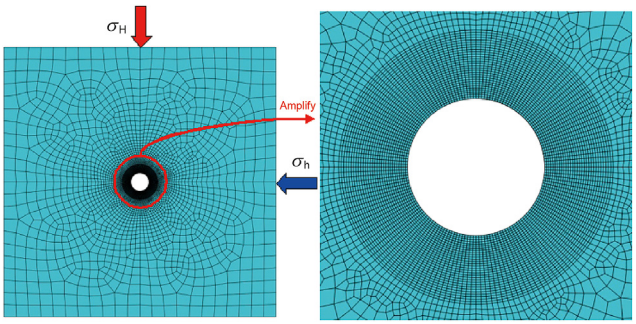

Fig. 6. Calculation model for a borehole under elastic-plastic damage of hard-brittle shale (σ_H and σ_h are the maximum and minimum horizontal *in situ* stresses, respectively).

Table 1
Calculation parameters.

Parameter	Value
Vertical depth	3000 m
Overburden pressure	69 MPa
Maximum horizontal *in situ* stress	65 MPa
Minimum horizontal *in situ* stress	45 MPa
Orientation of maximum horizontal *in situ* stress	N 0° E
Pore pressure	30 MPa
Elastic modulus	18000 MPa
Poisson's ratio	0.2

for wellbore stability analysis in fractured rock with the consideration of elastoplastic damage response.

A secondary development was initiated based on the ABAQUS finite-element package for numerical simulation studies. ABAQUS is a general purpose finite-element-analysis code that can analyze fluid seepage and mechanical problems in porous media and has been widely used to solve mechanical problems around a wellbore in recent years (Guo et al., 2016; Lin et al., 2017).

Based on the above method, a calculation model for elastic-plastic damage of hard-brittle shale is established, as shown in Fig. 6. On this basis, the mechanism of damage evolution of hard-brittle shale formations around a borehole after drilling is explored. The calculation parameters are displayed in Table 1.

Figs. 7–9 show the distribution law of normalized damage factors in the vicinity of a borehole after drilling with the drilling fluids of different densities. After drilling, the formation around the borehole does not fail when drilling fluids with these densities are used, and the borehole remains stable. However, due to a large concentration of stress, a certain area of the damaged zone appears around the borehole, and the maximum damage factor is found on the borehole wall at the orientation of the minimum horizontal *in situ* stress, indicating that the stress concentration is most significant at this position. The damaged zone showing the largest differences between the radial stress and circumferential stress mainly appears in the vicinity at the orientation of the minimum horizontal *in situ* stress, which is consistent with the fact that the major axis orientation of the elliptical borehole is parallel to the orientation of the minimum horizontal *in situ* stress when borehole instability occurs.

A damaged zone was found mainly around the formation at the orientation of the minimum horizontal *in situ* stress, where the difference between the radial stress and circumferential stress was the largest, which conformed to the fact that the orientation of the long axis of an ellipse-shaped borehole caused by collapse was parallel to that of the minimum horizontal *in situ* stress. Additionally, large scale stress damage appeared in the interior of the formation where the included angle with the orientation of the maximum horizontal *in situ* stress was approximately 45°. However, because the damaged zone was located in the interior of the formation, showing a nonsignificant stress concentration, the damage factors were all low, which had an insignificant influence on the physical properties of the formation.

The damage factor decreased with increasing distance to the wellbore wall. With increasing drilling time, the damage factor of the formation around the borehole gradually increased, while the increased amplitude gradually declined. After the borehole was completed for a certain period, the damage factor gradually stabilized. The increase in the damage factor was mainly due to drilling fluids flowing into the interior of the formation, thus resulting in an increase in the pore pressure of the formation around the borehole and a reduction in the radial effective stress.

The damage factors in these conditions were all smaller than 1, implying that the wellbore wall was still stable when the borehole was drilled under various drilling fluid densities. During drilling, a lower drilling fluid density corresponded to a larger damage factor at the site with the same distance to the wellbore wall. Moreover, the damage scope of the formation gradually expanded with the decrease in drilling fluid density, which indicated that a lower drilling fluid density corresponded to a higher damage degree of the formation around the borehole and easier borehole instability.

5. Evolution law of the permeability coefficient of hard-brittle shale around a borehole

Figs. 10–12 show the distribution law of the permeability coefficient in the vicinity of a borehole after drilling with different drilling fluid densities. After drilling, because the formation around the borehole was subjected to stress damage, microcracks occurred in the formation to further cause the permeability coefficient of the damaged zone to substantially increase, which is similar to the damaged zone where the permeability characteristics of the formation changed in the vicinity of the formation at the orientation of the minimum horizontal *in situ* stress. Within a certain zone where the included angle with the maximum horizontal *in situ* stress direction was 45°, the permeability coefficients also slightly increased. However, the permeability coefficient did not change significantly when the damage factor was low and its amplitude increased with an increasing damage degree. The permeability coefficient substantially changed only when the damage factor was larger than a certain value. Moreover, the total change range of the permeability coefficient was large. Therefore, the permeability coefficient of the formation at 45° (the nephogram in Fig. 9) failed to apply because the increase in the amplitude was quite low. With increasing drilling time, the permeability coefficient of the formation gradually increased, and the change range of permeability coefficients of the formation also gradually increased. After the borehole was drilled, the maximum permeability coefficient appeared in the wellbore wall at the orientation of the minimum horizontal *in situ* stress. Due to the heterogeneity of the *in situ* stress, the permeability of the formation around the borehole showed considerable anisotropism after the well was drilled. Moreover, the permeability of the formation at the orientation of the minimum horizontal *in situ* stress was far larger than that of the formation at the orientation of maximum horizontal *in situ* stress.

These figures show that a lower drilling fluid density during drilling corresponds to be a larger increase in the amplitude of the permeability coefficients of a formation. Moreover, the change range of the permeability increased with decreasing density of the drilling fluids. By taking the densities of the drilling fluids used in the study as an example, the permeability coefficient increased by at most 619 times when the borehole was drilled using a drilling

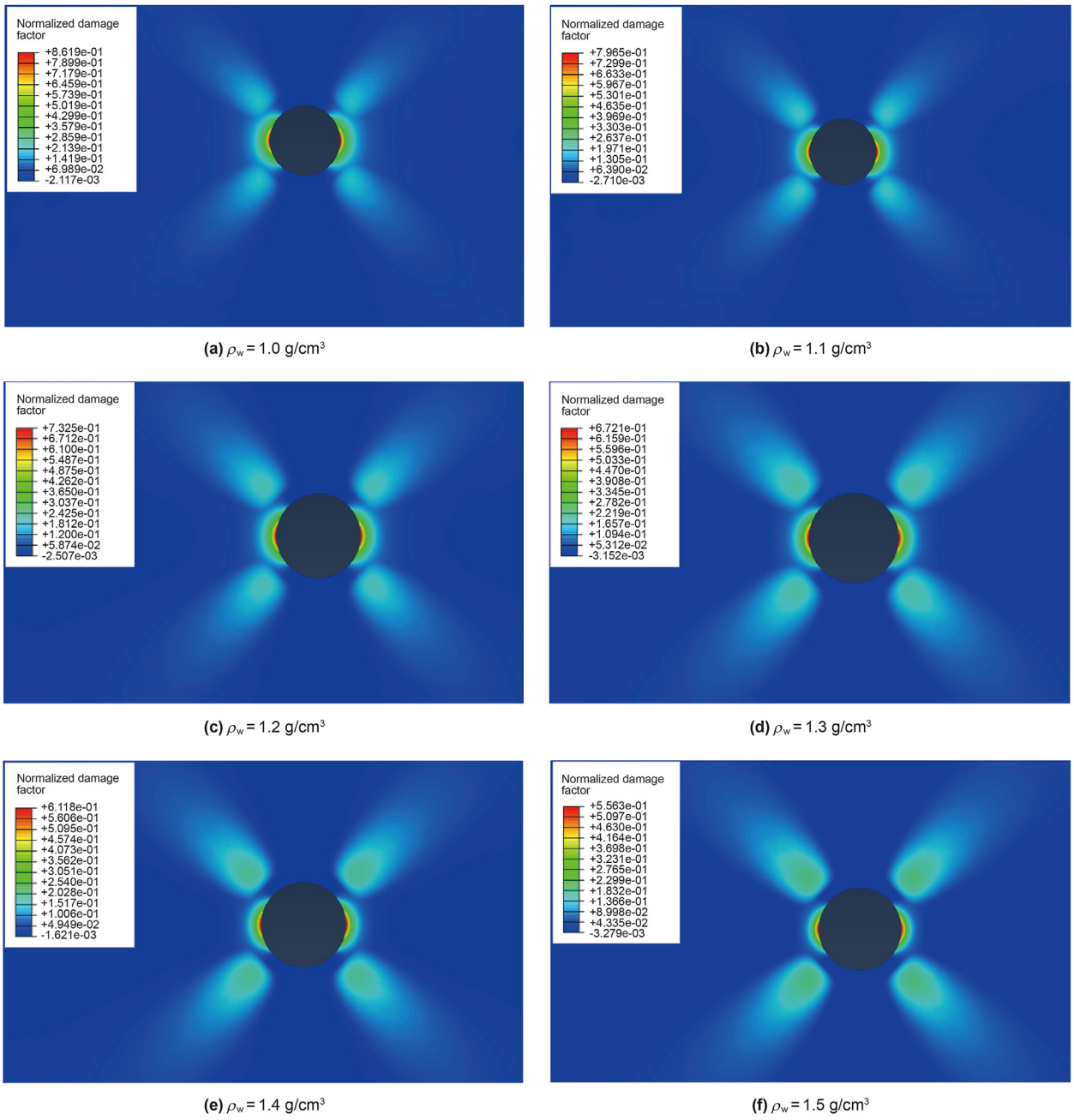

Fig. 7. Normalized damage factors of the formation around the borehole after drilling with drilling fluids of different densities (ρ_w is the drilling fluid density).

fluid with a density of 1.0 g/cm^3, while the permeability coefficient increased only 188 times when using a drilling fluid with a density of 1.5 g/cm^3. Because the permeability of the formation at the orientation of the maximum horizontal *in situ* stress remained unchanged, the anisotropism of the permeability of the formation around the borehole decreased substantially with the reduction in the density of the drilling fluids.

6. Borehole instability mechanism of hard-brittle shale

6.1. Critical drilling fluid density for borehole stability

Because borehole instability occurs at the orientation of the minimum horizontal *in situ* stress (Zoback et al., 1985; Yan et al., 2014), Fig. 13 presents the change law of the failure ratio of the formation around the borehole at the orientation of the minimum horizontal *in situ* stress with time when drilling with drilling fluids of six different densities. Based on the calculation results, a lower drilling fluid density corresponds to a larger failure ratio and more readily occurring borehole instability. The maximum failure ratio is always found in the borehole wall and gradually decreases toward the interior of the formation. Furthermore, greater proximity to the borehole wall corresponds to a faster decrease rate, and the ratio gradually tends to become stable in the formation, which indicates that borehole instability first appears in the borehole wall due to the greatest stress concentration in the borehole wall, the maximum circumferential stress and the minimum radial effective support.

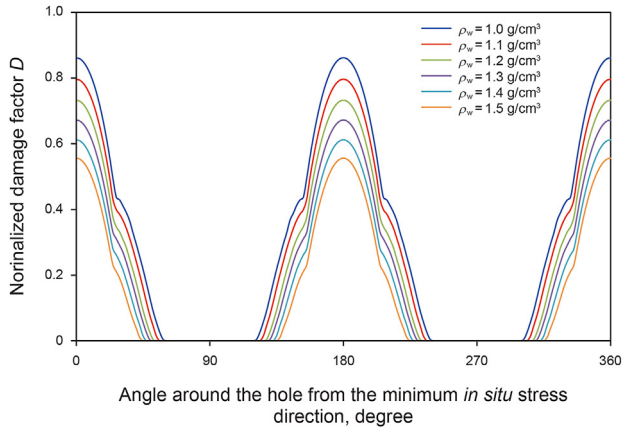

Fig. 8. Variation in the normalized damage factor at different orientations on the wellbore wall when different drilling fluid densities are used.

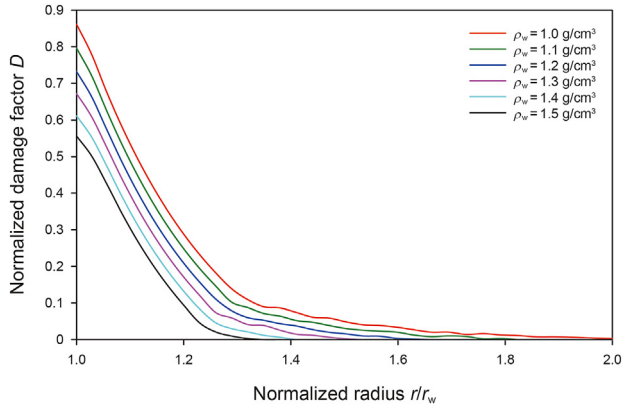

Fig. 9. The influence of drilling fluid density on the normalized damage factor along the direction of the minimum horizontal stress.

The failure ratio of the formation under the same density of drilling fluid is initially the minimum value after drilling and gradually increases with time after drilling. After the formation with an initial maximum failure ratio less than 1 is soaked in the drilling fluid for a certain time, the failure ratio may become equal to 1. In other words, the borehole wall that was initially able to remain stable after drilling may collapse after a period, that is the time effect of borehole collapse, because as the soaking time increases, the formation strength gradually decreases under the interaction of stress damage and soaking in the drilling fluid.

A smaller distance to the borehole wall corresponds to a greater stress concentration and a higher damage degree of the formation. Therefore, under the interaction of stress damage and soaking in the drilling fluid, the rate of decrease in formation strength is faster at positions closer to the borehole wall. As a result, the failure ratio of the formation at different distances from the borehole wall increases at different rates with time, and a smaller distance from the borehole wall corresponds to a faster increase rate for the failure ratio.

Fig. 14 shows the change law of the failure ratio in the borehole wall at the orientation of the minimum horizontal *in situ* stress, namely, the change law of the maximum failure ratio of the formation around the borehole with time after drilling with drilling fluids of six different densities. According to the calculation results, under all drilling fluid densities, the maximum failure ratios of the formation around the borehole increase with time. Immediately after drilling the borehole, the increase rate of the failure ratio is the maximum value and then gradually decreases. One week after completing the borehole, the failure ratios tend to be stable and barely change. The increase in the amplitudes of the failure ratios under different densities of drilling fluids with time varies considerably, and a lower drilling fluid density corresponds to a larger increase in the amplitude of the failure ratio with time mainly because a lower drilling fluid density corresponds to greater stress damage of the formation around the borehole and more significant strength of the formation decreases caused by seepage of the drilling fluid into the formation.

Fig. 15 displays the period of borehole collapse under different drilling fluid densities. Here, the period of borehole collapse is defined as the time from drilling to shear failure occurring of the borehole wall. The duration of the period of borehole collapse increases with increasing drilling fluid density. Under this calculation condition, when the density of the drilling fluid is less than 1.3 g/cm^3, although the borehole wall is stable in the early stage of drilling, the borehole wall will collapse within a very short time after drilling because of the rapid increase in the failure ratio. The period of borehole collapse is less than three days. Although the duration of the borehole collapse period increases with increasing drilling fluid density, the increase in the amplitude is very low; therefore, the increase in the density only slightly affects the period of borehole collapse. However, when the density of drilling fluid exceeds a certain value, the period of borehole collapse increases substantially. For example, when the density is 1.4 g/cm^3, the period of borehole collapse increases to 16 days, which is much longer than that when the density is 1.3 g/cm^3. When the density of the drilling fluid is 1.5 g/cm^3, the failure ratio is always smaller than 1; thus, the borehole remains stable for a long time and does not collapse.

A critical density of the drilling fluid is evident when drilling in hard-brittle shale. When the drilling fluid density is lower than this critical value, the borehole tends to be unstable after drilling over time, and any changes in the drilling fluid density have small influences on the improvement of borehole stability. However, when the drilling fluid density is higher than the critical value, the borehole stability increases considerably. Therefore, it is significant to evaluate the critical value of the drilling fluid density while drilling in hard-brittle shale.

6.2. Influence of the initial drilling fluid density on borehole stability

In drilling practice, the following situations can sometimes be encountered. When the borehole of a well collapses in hard-brittle shale, the density of the drilling fluid is increased to a certain value (for a convenient description, the density is denoted as ρ_m) to inhibit borehole collapse, thereafter the borehole wall stabilizes for a certain time and then collapses again. However, for an adjacent well, a drilling fluid with a density of ρ_m is used at the beginning of drilling in this formation, and the borehole can be stabilized for a very long time and may even never collapse. To explain this phenomenon, this study explored the change laws of the failure ratio of a formation around a borehole drilled initially using a drilling fluid with a low density (ρ_w = 1.0, 1.1, 1.2, 1.3, and 1.4 g/cm^3) and then using a drilling fluid with densities of 1.4 and 1.5 g/cm^3 after drilling has commenced. Fig. 16 shows the change law of the maximum failure ratio of the formation around a borehole with time after drilling. Fig. 17 demonstrates the period of borehole collapse using a drilling fluid with different initial densities and then changing to the same density after drilling.

When the initial density of the drilling fluid is low, the maximum failure ratio rapidly rises with drilling time, even if the

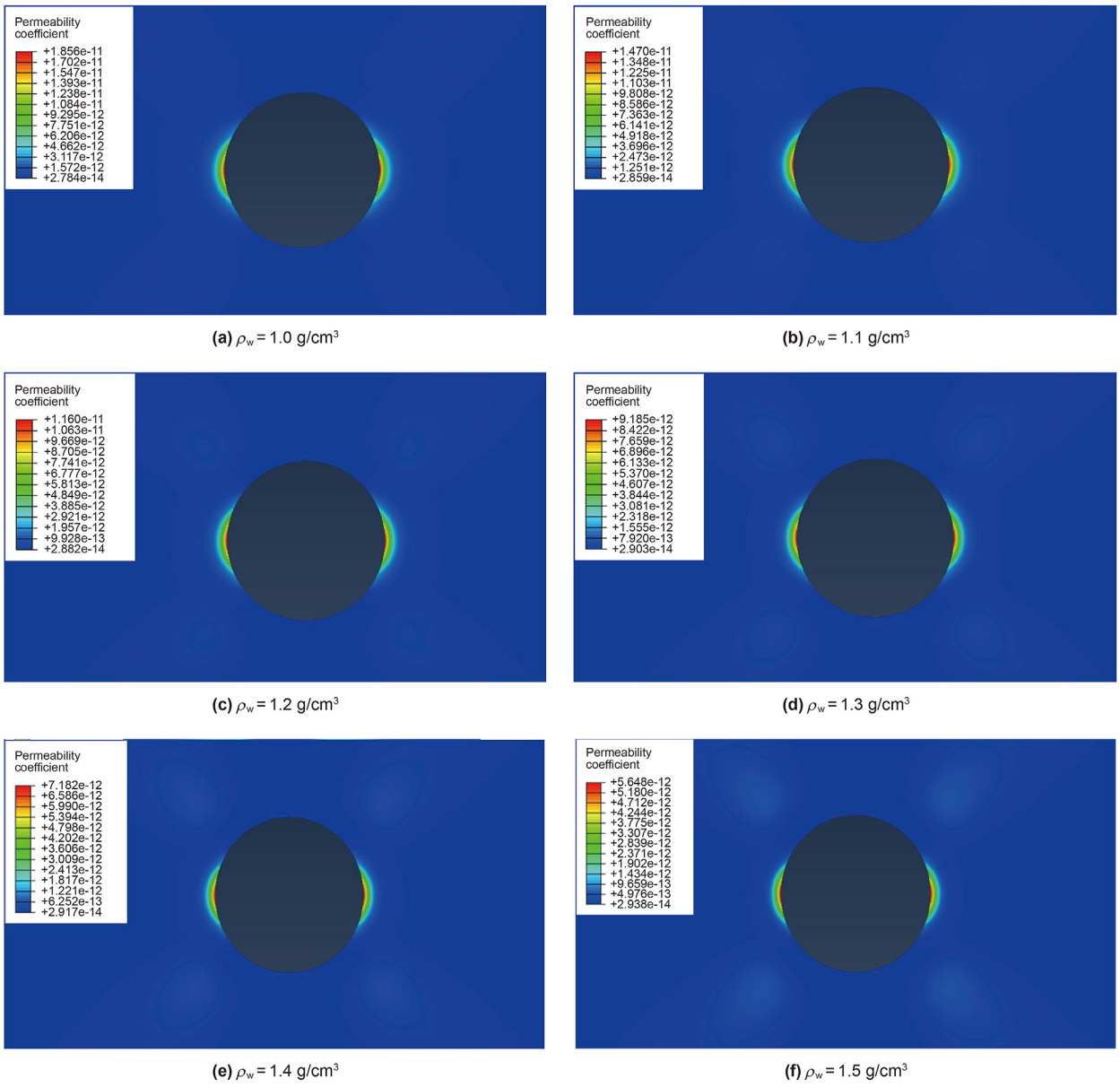

Fig. 10. Permeability coefficients of the formation around the borehole after drilling with drilling fluids of different densities.

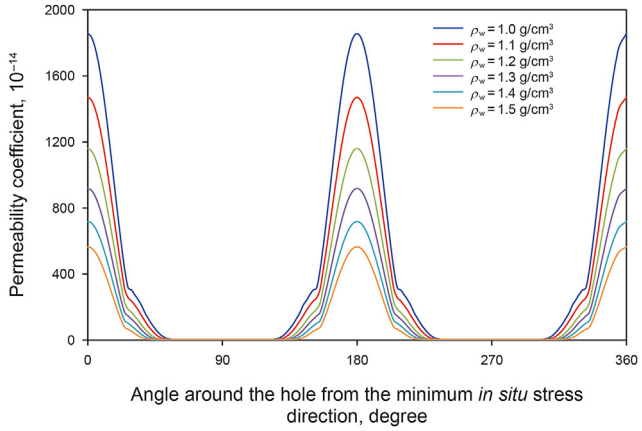

Fig. 11. Variation in the permeability coefficients at different orientations on the wellbore wall when different drilling fluid densities are used.

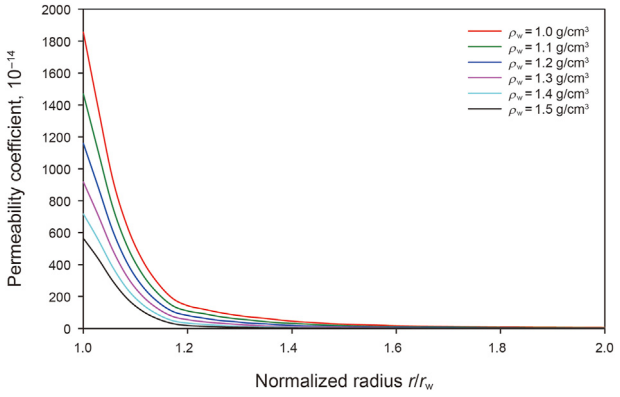

Fig. 12. The influence of mud densities on the permeability coefficients of the formation around the borehole at the orientation with the minimum horizontal *in situ* stress.

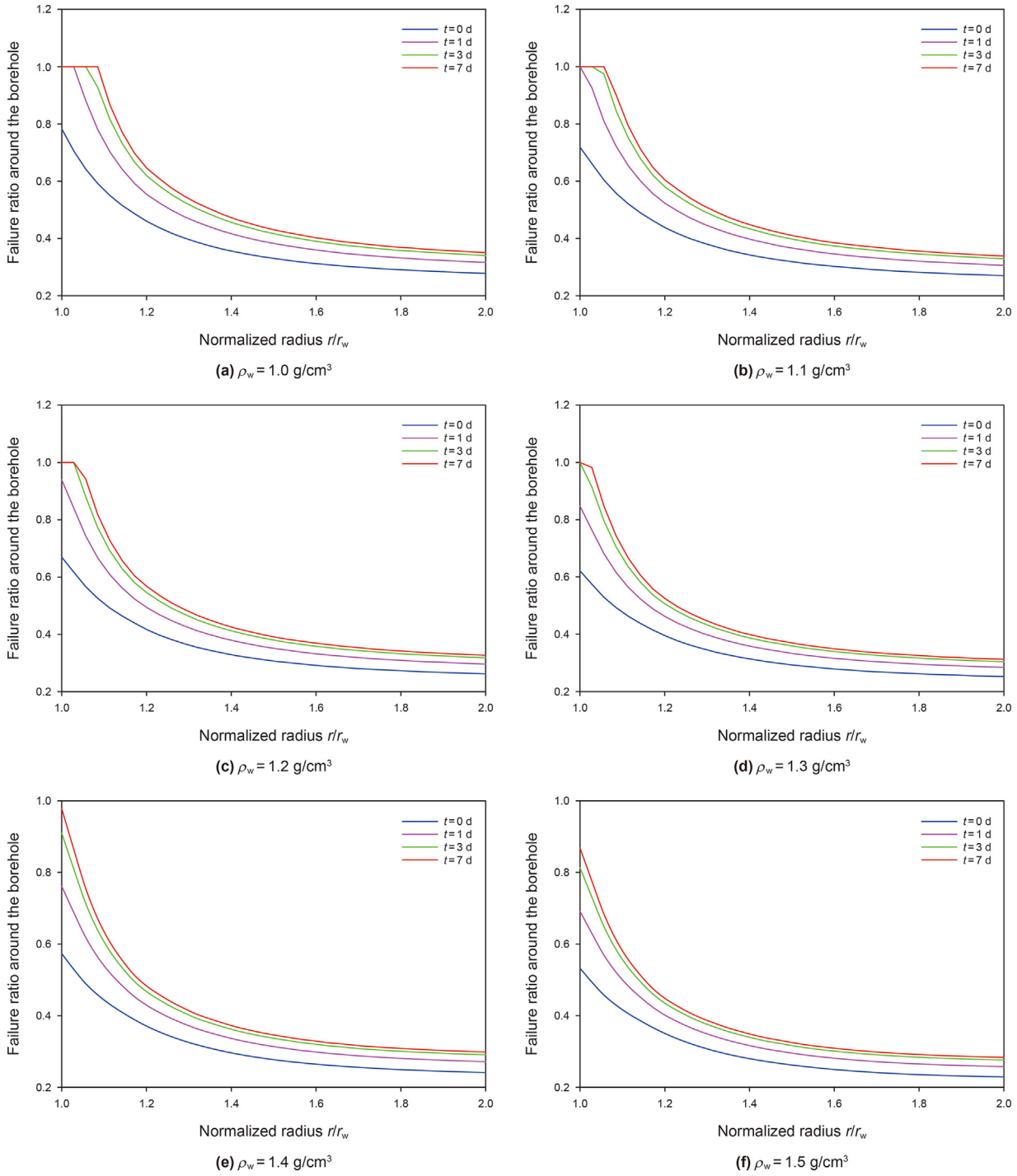

Fig. 13. Variation in the failure ratio around the borehole with drilling time.

drilling fluid is changed to a high-density drilling fluid after drilling. A lower initial drilling fluid density corresponds to a larger increase in the amplitude of the failure ratio and a shorter period of borehole collapse. For instance, when the drilling fluid with a density of 1.5 g/cm^3 is utilized in a later stage, if the initial density is smaller than 1.2 g/cm^3, the borehole collapses within five days, but the borehole can be stabilized for 16 days when the initial density is 1.3 g/cm^3, which is basically the same as the period of borehole collapse under the condition of drilling with a drilling fluid with a density of 1.4 g/cm^3 at all times, indicating that drilling fluids with densities of 1.4 and 1.5 g/cm^3 play the same role in stabilizing the borehole wall for a long period under these conditions. The main reason is that serious stress damage has occurred in the borehole wall when drilling fluid with a low density is used for drilling and the effect of the damage cannot be recovered. The damaged shale interacts with the drilling fluid, thereby substantially reducing the strength of the formation, and has little effect on whether the density of the drilling fluid is increased after drilling. Therefore, if the initial density of the drilling fluid is too low, it is difficult to maintain long-term stability of the borehole even though the drilling fluid is changed

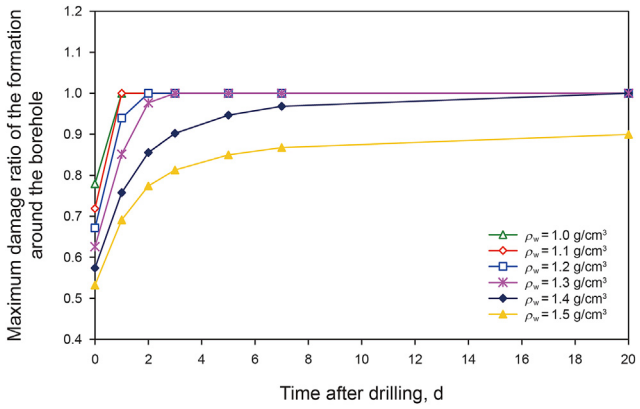

Fig. 14. Variation in the maximum failure ratio with drilling time and drilling fluid density.

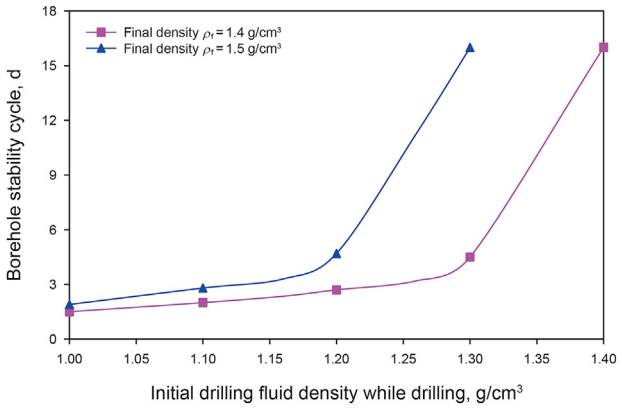

Fig. 17. Variation in the borehole stability cycle with different initial drilling fluid densities when the final density is the same.

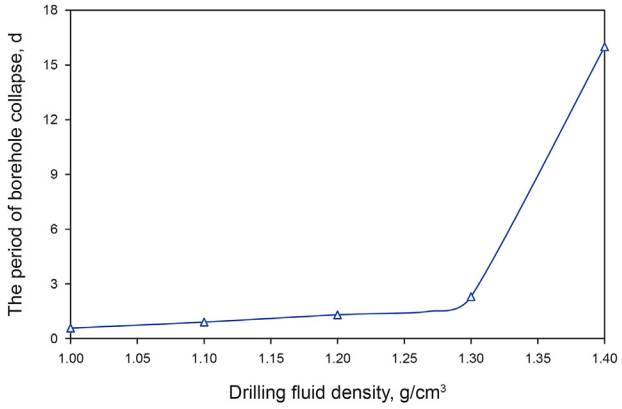

Fig. 15. Variation in the period of borehole collapse with drilling fluid density.

to a high-density drilling fluid after drilling.

This conclusion is consistent with the actual drilling conditions of hard-brittle shale in some oilfields, such as the Shahejie Formation in the Bohai Oilfield, China. A well in this oil field used a drilling fluid with a density of 1.22 g/cm^3 for drilling when the Shahejie Formation was had just been drilled. Later, due to collapse of the wellbore, the drilling fluid density was continuously increased to 1.45 g/cm^3, but damage had already occurred in the wellbore at this time. By increasing the drilling fluid density, although the borehole instability was suppressed in the short term, it quickly increased. When an adjacent well was drilled in the Shahejie Formation, 1.38 g/cm^3 drilling fluid was used, and then the drilling fluid density was quickly increased to 1.42 g/cm^3 and then to 1.45 g/cm^3. This well is relatively smooth throughout the drilling process, with almost no borehole instability.

Borehole instability of hard-brittle shale results from the interaction of stress damage and drilling fluid. Therefore, for hard-brittle shale formations that easily suffer borehole instability, a complete understanding of the mechanical characteristics of the formation and accurate prediction of the period of borehole collapse under different densities is required before practical drilling starts. Moreover, in the initial stage of drilling, a drilling fluid with a proper density should be used instead of increasing the density of the drilling fluid only after the borehole collapses, which is favorable for maintaining long-term borehole stability, improving drilling efficiency and maintaining safety in drilling.

7. Conclusions

(1) After drilling, although a borehole is stable, a certain area of damaged zone can be found in the vicinity of the borehole and is mainly concentrated in the formation near the borehole at the orientation of the minimum horizontal *in situ* stress.

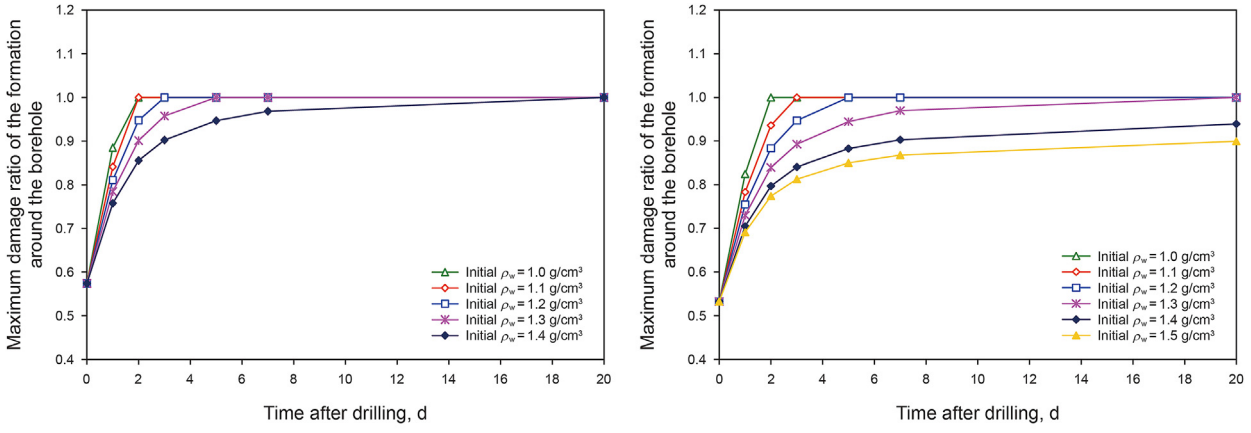

(a) Change in the drilling fluid density to 1.4 g/cm³ after drilling

(b) Change in the drilling fluid density to 1.5 g/cm³ after drilling

Fig. 16. Variation in the maximum failure ratio with different initial drilling fluid densities (changed to the same density after drilling).

(2) With increasing soaking time in the drilling fluid, the strength of hard-brittle shale gradually decreases. Greater stress damage corresponds to a larger decrease in the amplitude of the strength of the shale after soaking. The influence of the damage factor on the decrease in the amplitude of the strength increases with increasing damage factor. The uniaxial strength of cores that were not loaded before soaking and loaded to 30%, 60%, 80%, 95% of the uniaxial compressive strength was reduced by 12%, 14%, 18%, 29% and 52%, respectively, after 7 days of soaking.

(3) The maximum failure ratio of a formation around a borehole increases with increasing drilling time, and the borehole stability gradually becomes poorer. Even if a borehole is stable after a well is initially drilled, the borehole instability is likely to appear after a certain period. A lower drilling fluid density corresponds to faster increases in the failure ratio with time and a shorter period of borehole collapse. The drilling fluid has a critical density (1.3 g/cm^3 in this paper). When the drilling fluid density is lower than this critical value, the borehole tends to be unstable after drilling as time progresses, and any changes in the drilling fluid density have small influences on improvements in borehole stability. However, when the drilling fluid density is higher than the critical value, the borehole stability increases substantially.

(4) When the density of the drilling fluid initially used is extremely low, the formation around the borehole is subjected to serious stress damage. Although the drilling fluid is changed to a high-density drilling fluid after drilling, the failure ratio rapidly increases with drilling time, thus complicating the maintenance of long-term borehole stability. When a drilling fluid with a density of 1.5 g/cm^3 is utilized in a later stage, and if the initial density is smaller than 1.2 g/cm^3, the borehole collapses within 5 days, but the borehole can be stabilized for 16 days when the initial density is 1.3 g/cm^3, which is basically the same as the period of borehole collapse under the condition of drilling with a drilling fluid with a density of 1.4 g/cm^3 at all times. While drilling in hard-brittle shale formations, a proper initial density of the drilling fluid should be used rather than increasing the density of the drilling fluid only after the borehole collapses, which is beneficial to stabilization of the borehole for a long time.

(5) Borehole instability of hard-brittle shale results from reduced strength of a formation because drilling fluid infiltrates the interior after microcracks are generated in the formation around the borehole due to the stress damage caused by the concentration of stress in drilling. Any measures that can reduce the damage degree of a formation around a borehole and the influences of drilling fluid on microcracks are favorable for long-term borehole stability.

Acknowledgments

This work is financially supported by the National Natural Science Foundation Project of China (52074224, U1762216) and the Key Research and Development Program of Shandong Province (2019GGX103025).

References

Browning, W.C., Perricone, A.C., 1963. Clay chemistry and drilling fluids. Drilling and Rock Mechanics Symposium. https://doi.org/10.2118/540-MS.

Chen, G.Z., Chenevert, M.E., Sharma, M.M., et al., 2003. A study of wellbore stability in shales including poroelastic, chemical, and thermal effects. J. Petrol. Sci. Eng. 38 (3–4), 167–176. https://doi.org/10.1016/S0920-4105(03)00030-5.

Chen, M., Jin, Y., Zhang, G.Q., 2008. Petroleum Engineering Rock Mechanics. Science Press, Beijing.

Chenevert, M.E., 1970. Shale control with balanced-activity oil-continuous muds. J. Petrol. Technol. 22 (10), 1309–1316. https://doi.org/10.2118/2559-PA.

Dodson, J., Dodson, T., Schmidt, V., 2004. Gulf of Mexico 'trouble time' creates major drilling expenses: use of cost-effective technologies needed. Offshore 64 (1), 46–48.

Eberhardt, E., Stead, D., Stimpson, B., 1999. Quantifying progressive pre-peak brittle fracture damage in rock during uniaxial compression. Int. J. Rock Mech. Min. Sci. 36 (3), 361–380. https://doi.org/10.1016/S0148-9062(99)00019-4.

Fairhurst, C., Cook, N.G.W., 1966. The maximum phenomenon of rock splitting parallel to a free surface under compressive stress. The 1st Congress of the International Society of Rock Mechanics. ISRM-1CONGRESS-1966-115.

Gaede, O., Karrech, A., Regenauer-Lieb, K., 2013. Anisotropic damage mechanics as a novel approach to improve pre- and post-failure borehole stability analysis. Geophys. J. Int. 193 (3), 1095–1109. https://doi.org/10.1093/gji/ggt045.

Gao, J.J., Deng, J.G., Lan, K., et al., 2017a. Porothermoelastic effect on wellbore stability in transversely isotropic medium subjected to local thermal non-equilibrium. Int. J. Rock Mech. Min. Sci. 96, 66–84. https://doi.org/10.1016/j.ijrmms.2016.12.007.

Gao, J.J., Lau, H.C., Sun, J., 2020. A semianalytical poroelastic solution to evaluate the stability of a borehole drilled through a porous medium saturated with two immiscible fluids. SPE J. 25 (5), 2319–2340. https://doi.org/10.2118/195515-PA.

Gao, Y., Liu, Z.L., Zhuang, Z., Gao, D.L., Hwang, K.C., 2017b. Cylindrical borehole failure in a transversely isotropic poroelastic medium. J. Appl. Mech. 84 (11). https://doi.org/10.1115/1.4037880.

Ghassemi, A., Tao, Q., Diek, A., 2009. Influence of coupled chemo-poro-thermoelastic processes on pore pressure and stress distributions around a wellbore in swelling shale. J. Petrol. Sci. Eng. 67 (1–2), 57–64. https://doi.org/10.1016/j.petrol.2009.02.015.

Guo, T.K., Qu, Z.Q., Gong, D.G., et al., 2016. Numerical simulation of directional propagation of hydraulic fracture guided by vertical multi-radial boreholes. J. Nat. Gas Sci. Eng. 35, 175–188. https://doi.org/10.1016/j.jngse.2016.08.056.

Hajiabdolmajid, V., Kaiser, P., 2003. Brittleness of rock and stability assessment in hard rock tunneling. Tunn. Undergr. Space Technol. 18 (1), 35–48. https://doi.org/10.1016/S0886-7798(02)00100-1.

Hajiabdolmajid, V., Kaiser, P.K., Martin, C.D., 2002. Modelling brittle failure of rock. Int. J. Rock Mech. Min. Sci. 39 (6), 731–741. https://doi.org/10.1016/S1365-1609(02)00051-5.

Hale, A.H., Mody, F.K., Salisbury, D.P., 1993. The influence of chemical potential on wellbore stability. SPE Drill. Complet. 8 (3), 207–216. https://doi.org/10.2118/23885-PA.

Islam, M., Skalle, P., Faruk, A.M.M., et al., 2009. Analytical and numerical study of consolidation effect on time delayed borehole stability during underbalanced drilling in shale. In: Kuwait International Petroleum Conference and Exhibition. https://doi.org/10.2118/127554-MS.

Jia, S.P., 2009. Hydro-mechanical coupled creep damage constitutive model of Boom clay, back analysis of model parameters and its engineering application. Chin. J. Rock Mech. Eng. 28 (12), 2594, 2594 (in Chinese).

Jia, S.P., Cheng, W.Z., Yu, H.D., et al., 2009. Research on seepage-stress coupling damage model of Boom clay during tunneling. Rock Soil Mech. 30 (1), 19–26 (in Chinese).

Jiang, Z.Q., Ji, L.J., Zuo, R.S., et al., 2002. Correlativity among rock permeability and strain, stress under servo-control condition. Chin. J. Rock Mech. Eng. 21 (10), 1142–1446 (in Chinese).

Kanfar, M.F., Chen, Z., Rahman, S.S., 2015. Effect of material anisotropy on time-dependent wellbore stability. Int. J. Rock Mech. Min. Sci. 78, 36–45. https://doi.org/10.1016/j.ijrmms.2015.04.024.

Lin, B.T., Jin, Y., Chen, S.L., 2017. A criterion for evaluating the efficiency of water injection in oil sand reservoirs. J. Petrol. Sci. Eng. 149, 322–330. https://doi.org/10.1016/j.petrol.2016.10.056.

Liu, Y.S., Bai, J.Z., Huang, R.Z., et al., 1998. A study on stability of brittle shale wellbore. J. Acta Petrolei Sinica 19 (1), 85–88 (in Chinese).

Ma, J.J., Zhao, G.F., 2018. Borehole stability analysis in fractured porous media associated with elastoplastic damage response. Int. J. GeoMech. 18 (5), 04018022. https://doi.org/10.1061/(ASCE)GM.1943-5622.0001115.

Ma, T.S., Chen, P., 2015. A wellbore stability analysis model with chemical-mechanical coupling for shale gas reservoirs. J. Nat. Gas Sci. Eng. 26, 72–98. https://doi.org/10.1016/j.jngse.2015.05.028.

Mody, F.K., Hale, A.H., 1993. Borehole-stability model to couple the mechanics and chemistry of drilling-fluid/shale interactions. J. Petrol. Technol. 45 (11), 1093–1101. https://doi.org/10.2118/25728-PA.

Oda, M., Takemura, T., Aoki, T., 2002. Damage growth and permeability change in triaxial compression tests of Inada granite. Mech. Mater. 34 (6), 313–331. https://doi.org/10.1016/S0167-6636(02)00115-1.

Qiao, L., Gao, W., Li, Y., et al., 2012. Improved CWFS model for hard rocks and its application to stability analysis of high rock slope. Chin. J. Rock Mech. Eng. 31 (S1), 2593–2599 (in Chinese).

Renani, H.R., Martin, C.D., 2018. Cohesion degradation and friction mobilization in brittle failure of rocks. Int. J. Rock Mech. Min. Sci. 106, 1–13. https://doi.org/10.1016/j.ijrmms.2018.04.003.

Shao, J.F., Khazraei, R., 1994. Wellbore stability analysis in brittle rocks with continuous damage model. Rock Mech. Petrol. Eng. https://doi.org/10.2118/28054-MS.

Shen, X.P., Mroz, Z., Xu, B.Y., 2001. Constitutive theory of plasticity coupled with orthotropic damage for geomaterials. Appl. Math. Mech. 22 (9), 1028–1034.

https://doi.org/10.1007/BF02438321.
Souley, M., Homand, F., Pepa, S., et al., 2001. Damage-induced permeability changes in granite: a case example at the URL in Canada. Int. J. Rock Mech. Min. Sci. 38 (2), 297–310. https://doi.org/10.1016/S1365-1609(01)00002-8.
Su, G.Z., 2006. Study on Stability Analysis and Intelligent Optimization for Large Underground Caverns under High Geostress Condition.. PhD Thesis Institute of Rock & Soil Mechanics, The Chinese Academy of Sciences, Wuhan.
Tang, L., Yang, J., Wang, Y., Yang, Z., 2007. An analysis of the effect of fracture and damage mechanics on wellbore stability. J. Harbin Eng. Univ. 28 (6), 642–646 (in Chinese).
Walton, G., 2019. Initial guidelines for the selection of input parameters for cohesion-weakening-friction-strengthening (CWFS) analysis of excavations in brittle rock. Tunn. Undergr. Space Technol. 84, 189–200. https://doi.org/10.1016/j.tust.2018.11.019.
Wang, B.Y., Deng, J.G., Zou, L.Z., et al., 2006. Applied research of collapse cycle of shale in wellbore using a coupled physico-chemical model. Acta Pet. Sin. 27 (3), 130–132 (in Chinese).
Wang, Q., Zhou, Y.C., Wang, G., et al., 2012. A fluid-solid-chemistry coupling model for shale wellbore stability. Petrol. Explor. Dev. 39 (4), 508–513. https://doi.org/10.1016/S1876-3804(12)60069-X.
Wang, W., Deng, J.G., Yu, B.H., et al., 2016a. Coupled effects of stress damage and drilling fluid on strength of hard brittle shale. J. Cent. S. Univ. 23 (12), 3256–3261. https://doi.org/10.1007/s11771-016-3391-7.
Wang, Y.L., Liu, Z.L., Yang, H.L., et al., 2016b. FE analysis of rock with hydraulic-mechanical coupling based on continuum damage evolution. Math. Probl Eng. https://doi.org/10.1155/2016/8534965, 2016.
Wang, Y.L., Liu, Z.L., Yang, H.L., et al., 2017a. Finite element analysis for wellbore stability of transversely isotropic rock with hydraulic-mechanical-damage coupling. Sci. China Technol. Sci. 60 (1), 133–145. https://doi.org/10.1007/s11431-016-0007-3.
Wang, Y.L., Zhuang, Z., Liu, Z.L., et al., 2017b. Finite element analysis for inclined wellbore stability of transversely iso-tropic rock with HMCD coupling based on weak plane strength criterion. Sci. China Technol. Sci. https://doi.org/10.1007/s11431-016-0460-2.
Yan, C.L., 2014. Borehole Instability Mechanism of Hard Brittle Shale.. PhD Thesis China University of Petroleum, Beijing.
Yan, C.L., Cheng, Y.F., Deng, F.C., et al., 2017a. Characteristics of stress damage and seepage of shale during drilling. In: 4th ISRM Young Scholars Symposium on Rock Mechanics.
Yan, C.L., Deng, J.G., Cheng, Y.F., et al., 2017b. Mechanical properties of gas shale during drilling operations. Rock Mech. Rock Eng. 50 (7), 1753–1765. https://doi.org/10.1007/s00603-017-1203-5.
Yan, C.L., Deng, J.G., Hu, L.B., et al., 2015. Brittle failure of shale under uniaxial compression. Arabian J. Geosci. 8 (5), 2467–2475. https://doi.org/10.1007/s12517-014-1373-3.
Yan, C.L., Deng, J.G., Yu, B.H., et al., 2014. Borehole stability in high-temperature formations. Rock Mech. Rock Eng. 47 (6), 2199–2209. https://doi.org/10.1007/s00603-013-0496-2.
Yang, S.Y., Yu, M.H., Fan, S.C., 2000. An elasto-plastic damage model for saturated and unsaturated geomaterials. Acta Mech. Sin. 32 (2), 198–206. https://doi.org/10.1016/j.clay.2016.09.009 (in Chinese).
Yew, C.H., Chenevert, M.E., Wang, C.L., et al., 1990. Wellbore stress distribution produced by moisture adsorption. SPE Drill. Eng. 5 (4), 311–316. https://doi.org/10.2118/19536-PA.
Yu, M., Chen, G., Chenevert, M.E., et al., 2001. Chemical and thermal effects on wellbore stability of shale formations. In: SPE Annual Technical Conference and Exhibition. https://doi.org/10.2118/71366-MS.
Zeynali, M.E., 2012. Mechanical and physico-chemical aspects of wellbore stability during drilling operations. J. Petrol. Sci. Eng. 82, 120–124. https://doi.org/10.1016/j.petrol.2012.01.006.
Zhang, F.F., Kang, Y.F., Wang, Z.Y., et al., 2018. Transient coupling of swab/surge pressure and in situ stress for wellbore-stability evaluation during tripping. SPE J. 23 (4), 1019–1038. https://doi.org/10.2118/180307-PA.
Zhang, J.C., Lang, J., Standifird, W., 2009. Stress, porosity, and failure-dependent compressional and shear velocity ratio and its application to wellbore stability. J. Petrol. Sci. Eng. 69 (3–4), 193–202. https://doi.org/10.1016/j.petrol.2009.08.012.
Zheng, G., 2005. Research on the Damage and Fracture Mechanism of Wellbore Stability. Ph.D. Thesis. Harbin: Harbin Engineering University.
Zhou, J., He, S.M., Tang, M., et al., 2018. Analysis of wellbore stability considering the effects of bedding planes and anisotropic seepage during drilling horizontal wells in the laminated formation. J. Petrol. Sci. Eng. 170, 507–524. https://doi.org/10.1016/j.petrol.2018.06.052.
Zoback, M.D., Moos, D., Mastin, L., et al., 1985. Well bore breakouts and in situ stress. J. Geophys. Res. Solid Earth 90 (B7), 5523–5530. https://doi.org/10.1029/JB090iB07p05523.